NAIC-ID(RS)T-0638-95

# NATIONAL AIR INTELLIGENCE CENTER

A STUDY OF TECHNOLOGY FOR DETECTION OF NONLUMINOUS ARTIFICIAL SATELLITES IN DAYLIGHT

by

He Cheng, Zhu Qixiang



19960221 091

NAIC- ID(RS)T-0638-95

# HUMAN TRANSLATION

NAIC-ID(RS)T-0638-95 21 December 1995

MICROFICHE NR: 95C000789

A STUDY OF TECHNOLOGY FOR DETECTION OF NONLUMINOUS ARTIFICIAL SATELLITES IN DAYLIGHT

By: He Cheng, Zhu Qixiang

English pages: 11

Source: Unknown

Country of origin: China
Translated by: Edward A. Suter
Requester: NAIC/TASC/John L. Gass
Approved for public release: distribution unlimited.

| THIS TRANSLATION IS A RENDITION OF THE ORIGINAL FOREIGN TEXT WITHOUT ANY ANALYTICAL OR EDITORIAL COMMENT STATEMENTS OR THEORIES ADVOCATED OR IMPLIED ARE THOSE OF THE SOURCE AND DO NOT NECESSARILY REFLECT THE POSITION OR OPINION OF THE NATIONAL AIR INTELLIGENCE CENTER. | PREPARED BY:<br><br>TRANSLATION SERVICES<br>NATIONAL AIR INTELLIGENCE CENTER<br>WPAFB, OHIO |
|---|---|

GRAPHICS DISCLAIMER

All figures, graphics, tables, equations, etc. merged into this translation were extracted from the best quality copy available.

*China Astronautics and Missilery Abstracts*
Vol. 1, Issue 4, 1993

# A STUDY OF TECHNOLOGY FOR DETECTION OF NONLUMINOUS ARTIFICIAL SATELLITES IN DAYLIGHT

(Romanized title: "*Baitian Feizifaguang Tianti Mubiao Tance Jishu De Yanjiu*")

by He Cheng and Zhu Qixiang (Academia Sinica, Photoelectric Technology Institute, Chengdu 610209)

**Abstract:** In this paper, the authors discuss the detection limits of systems for detecting nonluminous artificial satellites in daylight, as well as the relationship of target contrast and signal-to-noise ratio to artificial satellite characteristics, sky background characteristics, optical system parameters, and CCD [charge-coupled device] parameters. The authors discuss in depth the effects of spectral filtering technology on detection limits, contrast, and signal-to-noise ratio. Results of numerical simulations demonstrate that spectral filtering technology can increase the target satellite's optical contrast by 4 to 8 times, raise the target satellite's signal-to-noise ratio by 1.5 to 2.5 times, and enhance the system's limit detection brightness by 0.4 to 0.7 visual magnitude.

## Foreword

Detection of signals from low-contrast, weak targets that reflect sunlight in daytime when background signals are strong is a key technology for optical and photoelectric detection, tracking, and measurement of nonluminous artificial satellites. During the daytime, when the sky is bright, background signals are strong and artificial satellites shine by reflecting sunlight. The spectral characteristics of artificial satellites are similar to those of their backgrounds. Thus, it is necessary first to solve the technical problems of extracting the signals of artificial satellites from intense background signals when carrying out detection during the daytime. The methods that are often used today to solve this problem include:

(1) Adopting refrigeration technology to reduce the device's thermal noise;

(2) Using a low-noise, wide-band pre-amplifier to amplify the photoelectric detector's output signal. This method can only prevent noise from expanding, and has no suppressing effect on the noise already produced by the detector;

(3) Employing relevant techniques to suppress noise and increase the output signal-to-noise ratio. Using correlated dual-sampling circuits lowers the charge-coupled device's reset noise, but cannot lower its shot noise;

(4) Adopting self-adaptive background suppression methods to suppress sky background signals. These methods cannot reduce the shot noise created by background photon fluctuation, either.

In this paper, we advance an optical method of reducing background radiation: spectral wave filtering technology. This method reduces background photon radiation, radically lowers the system's noise — especially photon shot noise — and raises the system's signal-to-noise ratio.

## 1 Artificial satellite spectrum characteristics and background characteristics

**1.1 Artificial satellite spectrum characteristics** Artificial satellites are not usually self-luminous. The sun shines on them in the upper atmosphere and they reflect the sun's light. The intensity of illumination of spheroids [viewed] from the earth's surface can be calculated using the following formula:

$$E(\lambda) = \tau(\lambda)^{SEC(Z)} \cdot \rho(\lambda) \cdot E_0(\lambda) \cdot [(2 \cdot R^2/3 \cdot ((\pi - \beta) \cdot COS(\beta) + SIN(\beta))]/(\pi \cdot L^2) \qquad (1)$$

Page 29

Here, $Z$ is the zenith angle, $\rho(\lambda)$ is the spectral reflectivity of the spheroid's surface, $R$ is the radius of the spheroid, $\beta$ is the phase angle (the included angle between the sun, the target, and the detector), $L$ is the target's apparent distance, and $E_0$ is the sun's intensity of illumination outside the atmosphere.

The surface paint colors of targets being detected are either white or green. The spectral illumination characteristics (obtained through numerical calculation) of targets viewed from the earth are shown in Figure 1.

**1.2 Background spectral characteristics** During the day, the sky is bright. Its luminance ranges from 0.1 to 1 stilb[1]. Its spectral irradiance characteristics are shown in Figure 1. One can tell from Figure 1 that background radiation is primarily concentrated in the 0.2 - 0.6 μm wave band, and artificial satellite radiation is in the small wave band from 0.2 - 0.4 μm. This provides conditions for the application of spectral wave filtering technology.

## 2. Analysis of spectral filtering technology and contrast

Spectral filtering technology is the choosing of an appropriate wave filter based on the difference between the spectral radiation from the artificial satellite being detected and the spectral radiation from its background. It causes light radiation entering the photoelectric receiver to be limited to necessary wavelengths, and reduces background radiation photons received by the photoelectric receiver to the greatest extent possible, thus raising target-signal contrast and signal-to-noise ratio.

The definition of the target artificial satellite's optical contrast C[2] is the ratio between the spectral radiant luminance $L_S$ of the target on the detector's surface to the spectral radiant luminance of the background $L_B$, i.e.:

$$C = L_S/L_B \tag{2}$$

It can be proved that the optical contrast given in the above definition is equivalent to that in the formulas below:

$$C = H_S/H_B \tag{3}$$

$$= \frac{\int_{\lambda_1}^{\lambda_2} E_S(\lambda) \cdot \tau_{大}(\lambda) \cdot \tau_F(\lambda) d\lambda}{\int_{\lambda_1}^{\lambda_2} E_B(\lambda) \cdot \tau_{大}(\lambda) \cdot \tau_F(\lambda) d\lambda} \tag{4}$$

In these formulas, $H_S$ and $H_B$ are, respectively, the integral illumination of the artificial satellite and of its background; $\tau_{*}$ is the optical system's spectral penetration rate; $E_S$ and $E_B$ are, respectively, the spectral illumination of the target and its background at the optical system's entrance pupil; and $\tau_F$ is the light filter's spectral penetration rate.

If $\lambda_0$ is used to express the cutoff wavelength of the spectral light filter, and when $\lambda > \lambda_0$, then $\tau_F = 1$, and when $\lambda < \lambda_0$, then $\tau_F = 0$, clearly, choosing a light filter with an appropriate spectral penetration rate according to differences in the spectral distribution of the target and its background causes $\tau_F$ to have different effects on the target and its background. Choosing an appropriate photoelectric detector allows the spectral response of the detector to match the light filter's penetration rate characteristics, so that the highest amount of background suppression may be attained. In this way, elevation of the target's signal contrast is achieved.

Page 30

## 3. The relationship between contrast and signal-to-noise ratio

The photoelectric detectors that nonluminous artificial satellite photoelectric detection systems can use have CCD area array devices and silicon target-intensification camera tubes. Today, most use CCD area array devices. Below, the detection performance of photoelectric systems is calculated using CCD area array detectors as photoelectric receivers.

**3.1 Calculation of signal-to-noise ratio** The detection performance of photoelectric systems is often defined as the signal-to-noise ratio of the system's output signals. Signal-to-noise ratio is defined as:

$$SNR = I_S / \overline{(I_N^2)}^{1/2} \tag{5}$$

In this formula, $I_S$ represents the signal current of a CCD pixel, and represents the mean-root-square value of the noise current of a CCD pixel. $I_S$ can be written as[4]:

$$I_S = N_S \cdot f_H \cdot e \tag{6}$$

In this formula, $f_H$ represents the pixel's scanning frequency, $e$ is the electron's quantity of electric charge, and $N_S$ is the electric charge quantity of a signal output by a CCD pixel. $N_S$ can be obtained using the following formula[4]:

$$N_S = H_S \cdot Q_S \cdot S \cdot A \cdot T_S \cdot K/e \tag{7}$$

In this formula, $A$ is the system's entrance pupil point, $S$ is the sensitivity of the CCD, $H_S$ is the signal light's integral illumination, $Q_S$ is the quantum efficiency of the CCD to the signal light, $T_S$ is the signal light's integral time, and $K$ is the penetration rate of a neutral light filter.

The CCD's noise sources can be summed up as follows: shot noise, transfer noise, and thermal noise.

Thus, $\overline{(I_N^2)}^{1/2}$ can be written as:

$$\overline{(I_N^2)}^{1/2} = \overline{(I_{N1}^2} + \overline{I_{N2}^2} + \overline{I_{N3}^2})^{1/2} \tag{8}$$

1. Shot noise

The randomness of incident photon current produces incident photon shot noise. The mean square current of shot noise produced by signal current $I_S$, background current $I_B$, and dark current $I_D$ is a function of the CCD detector band $\Delta f$. Its expression is[5]:

$$\overline{I_{N1}^2} = 2 \cdot e \cdot (I_S + I_B + I_D) \cdot \Delta f \tag{9}$$

Because each pixel of the CCD can be seen as an integral wave filter with integral time $T$, its bandwidth is[5]:

$$\Delta f = 1/(2 \cdot T) \tag{10}$$

The background current from a pixel of a CCD can be written as[4]:

$$I_B = N_B \cdot f_H \cdot e \tag{11}$$

In this formula, $N_B$ is the background quantity of electric charge from a CCD pixel. $N_B$ can be written as[4]:

$$N_B = H_B \cdot Q_B \cdot S \cdot A \cdot T_B \cdot A_P \cdot K/e \tag{12}$$

In this formula, $H_B$ is the integral intensity of background light, $Q_B$ is the quantum efficiency of the CCD to background light, $T_S$ is the integral time of background light, and $A_P$ is the angle area of a CCD pixel.

Because dark current $I_D << I_B$, when we do not consider the shot noise produced by dark current, $\overline{I_{N1}^2}$ can be expressed as:

$$\overline{I_{N1}^2} = e \cdot (I_S + I_B)/T \tag{13}$$

2. Transfer noise

The kind of transfer noise that has the greatest effect is transfer loss noise, which is also a kind of shot noise. It is primarily produced by $I_S$ and $I_B$. The mean square current of this kind of shot noise is[4]:

Page 31

$$\overline{I_{N2}^2} = (e \cdot I_B + e \cdot I_B) \cdot 2\varepsilon N/T \tag{14}$$

where $\varepsilon N$ represents the overall transfer loss rate following $N$ transfers. In general, $\varepsilon N = 0.1$.

3. Thermal noise

Because thermal noise is much fainter than shot noise, we will omit thermal noise here.

The system's signal-to-noise ratio can be expressed as:

$$SNR = I_s/(\overline{I_N^2})^{1/2} = \frac{H_S \cdot A \cdot Q_S \cdot S \cdot T_S \cdot K}{[e \cdot S \cdot A \cdot K \cdot 1.2(H_S \cdot Q_S \cdot T_S + H_B \cdot Q_B \cdot T_B \cdot A_P)]^{1/2}}$$

When detecting artificial satellites against a clear daylight background, because $H_S \ll H_B$ and $T_S \leq T_B$, signal-to-noise ratio can be simplified to:

$$SNR = \frac{H_S \cdot Q_S \cdot T_S \cdot (A \cdot S \cdot K)\ 1/2}{(e \cdot 1.2 \cdot H_B \cdot Q_B \cdot T_B \cdot A_P)\ 1/2} \tag{15}$$

**3.2 The relationship between contrast and signal-to-noise ratio** Assuming that the brightness of the sky background is definite, from formula (3) we can obtain:

$$H_S = C \cdot H_B \tag{16}$$

and because $T_B = T$, therefore:

$$SNR = \frac{C \cdot Q_S \cdot T_S \cdot (H_B \cdot S \cdot A \cdot K)\ 1/2}{(e \cdot 1.2 \cdot Q_B \cdot T \cdot A_P)\ 1/2} \tag{17}$$

When the background brightness detected by the detector surface is definite, the artificial

satellite's signal-to-noise ratio forms a direct ratio with its optical contrast.

## 4. An analysis of the detection capabilities of photoelectric detection systems

Detection capability is an important problem that must be solved first in photoelectric detection systems. The detection capability of photoelectric detection systems is decided by the following factors[6]:

(1) The artificial satellite's overall dimension, its surface reflectivity, and the altitude of its orbit;

(2) The zenith angle, phase angle, and background conditions when observing the artificial satellite;

(3) The optical system's parameters (caliber, penetration rate, relative aperture, etc.) and the spectral filter's cutoff wavelength;

(4) Functions of the receiver (spectrum corresponds to quantum efficiency, saturation electron number, etc.).

According to the Poisson distribution, when assured that SNR = 6 in 95% of detection probability, by using formula (15) we can obtain:

$$H_S = \frac{6 \cdot (1.2 \cdot e \cdot H_B \cdot Q_B \cdot T \cdot A_P)\,1/2}{Q_S \cdot T_S(S \cdot A \cdot K)\,1/2} \qquad (18)$$

After finding the target's $H_S$, it can be changed into the target's visual magnitude $M_V$. The results of numerical calculations show that spectral wave filter technology is effective at raising the system's limits of detection. Without using spectral wave technology, where SNR = 6, the CCD's saturation electron number is 130 K, telescope diameter D = 400 mm, background luminance is 5.1 stellar magnitudes, and the artificial satellite surface is painted white, gray, or black, the dimmest detectable artificial satellite is 6.6 stellar magnitudes; however, when a spectral wave filter with cutoff wavelength of 0.5 μm is added, the dimmest detectable artificial satellite is 7.0 magnitudes. When the artificial satellite surface is painted green, without spectral wave filter technology, the dimmest detectable target is 6.4 stellar magnitudes; but when a spectral wave filter with cutoff wavelength of 0.5 μm is added, the dimmest detectable target is

6.9 stellar magnitudes, and when a spectral wave filter with cutoff wavelength of 0.7 μm is added, the dimmest target the system can detect is 7.1 stellar magnitudes. Clearly, spectral wave filter technology can effectively suppress background photon radiation, and thus raise the system's detection limits.

Page 32

## 5. Numerical calculations

Four surface paint colors were used as examples: white, green, gray, and black[7]. Numerical calculations were carried out based on their surface reflectivity data. The results are displayed in figures 2, 3, and 4. In these figures, $\lambda_0$ represents the cutoff wavelength of the spectral wave filter. Conditions where $\lambda_0 = 0.2$ μm are equivalent to conditions where spectral wave filters are not used. We can tell from the figures that no matter what color the target is painted, using spectral wave filter technology can markedly improve the contrast and signal-to-noise ratio of the target's signals, and can raise the detection limits of photoelectric detection systems. Calculation results are shown in tables 1, 2, and 3.

## 6. Conclusions

Results of numerical calculation show that spectral wave filter technology is effective at enhancing the artificial-satellite detection capabilities of visible light detection systems in daylight. When detecting nonluminous artificial satellites, satellites' optical contrast can be multiplied by 4 to 8 times, and their signal-to-noise ratio can be multiplied by 1.5 to 2.5 times. In conditions where the system's parameters are definite, the system's limit detection magnitude can be raised by 0.4 to 0.7 visual magnitude.

① 表 1 ② 波长单位 : μm

| | $\lambda_0$ | 0.2 | 0.3 | 0.4 | 0.5 | 0.6 | 0.7 | 0.8 | 0.9 |
|---|---|---|---|---|---|---|---|---|---|
| ③ 对比度 | ④ 白漆 | 0.004 | 0.0059 | 0.0081 | 0.010 | 0.013 | 0.015 | 0.018 | 0.019 |
| | ⑤ 绿漆 | 0.0038 | 0.005 | 0.0068 | 0.0097 | 0.013 | 0.02 | 0.029 | 0.033 |
| | ⑥ 灰漆 | 0.0041 | 0.0059 | 0.0081 | 0.010 | 0.0122 | 0.0144 | 0.0166 | 0.0173 |
| | ⑦ 黑漆 | 0.0039 | 0.0058 | 0.0078 | 0.0098 | 0.0122 | 0.0149 | 0.0178 | 0.0194 |

Key: (1). Table 1. (2). Wavelength unit: μm. (3). Contrast. (4). Painted white. (5). Painted green. (6). Painted gray. (7). Painted black.

① 表 2 ② 波长单位:μm

| $\lambda_0$ | | 0.2 | 0.3 | 0.4 | 0.5 | 0.6 | 0.7 | 0.8 | 0.9 |
|---|---|---|---|---|---|---|---|---|---|
| ③ 信噪比 | ④ 白漆 | 2.4 | 2.9 | 3.43 | 3.7 | 3.5 | 2.8 | 2.0 | 1.3 |
| | ⑤ 绿漆 | 2.1 | 2.5 | 2.9 | 3.3 | 3.5 | 3.9 | 3.4 | 2.3 |
| | ⑥ 灰漆 | 2.4 | 2.96 | 3.43 | 3.61 | 3.4 | 2.79 | 1.93 | 1.2 |
| | ⑦ 黑漆 | 2.3 | 2.87 | 3.3 | 3.52 | 3.39 | 2.89 | 2.07 | 1.33 |

Key: (1). Table 2. (2). Wavelength unit: μm. (3). Signal-to-noise ratio. (4). Painted white. (5). Painted green. (6). Painted gray. (7). Painted black.

Page 33

① 表 3 ② 单位:目视星等

| $\lambda_0$ | | 0.2 | 0.3 | 0.4 | 0.5 | 0.55 | 0.6 | 0.7 | 0.8 |
|---|---|---|---|---|---|---|---|---|---|
| ③ 探测极限 | ④ 白漆 | 6.6 | 6.7 | 6.9 | 7.0 | 7.0 | 6.9 | 6.8 | 6.4 |
| | ⑤ 绿漆 | 6.4 | 6.5 | 6.8 | 6.9 | 6.9 | 7.0 | 7.1 | 6.9 |
| | ⑥ 灰漆 | 6.6 | 6.7 | 6.9 | 7.0 | 7.0 | 6.9 | 6.7 | 6.3 |
| | ⑦ 黑漆 | 6.6 | 6.7 | 6.9 | 7.0 | 7.0 | 6.7 | 6.7 | 6.4 |

Key: (1). Table 3. (2). Unit: Visual magnitude. (3). Detection limit. (4). Painted white. (5). Painted green. (6). Painted gray. (7). Painted black.

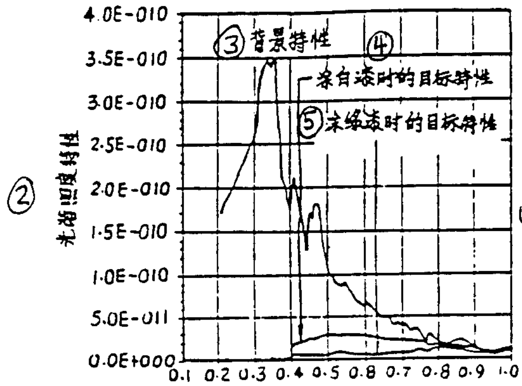


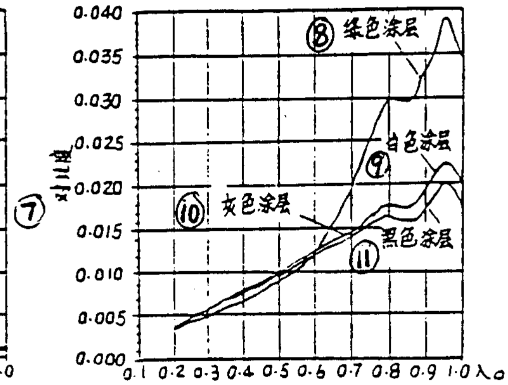


① 图 1 目标和背景的光谱照度特性

⑥ 图 2 对比度与 $\lambda_0$ 的关系

**Key:** (1). Figure 1. Spectral intensity of the target and its background. (2). Spectral intensity. (3). Background characteristics. (4). Characteristics of the target when painted white. (5). Characteristics of the target when painted green. (6). Figure 2. The relationship between contrast and $\lambda_0$. (7). Contrast. (8). Painted green. (9). Painted white. (10). Painted gray. (11). Painted black.

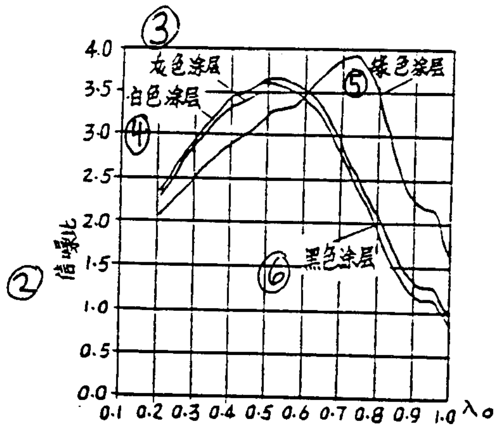


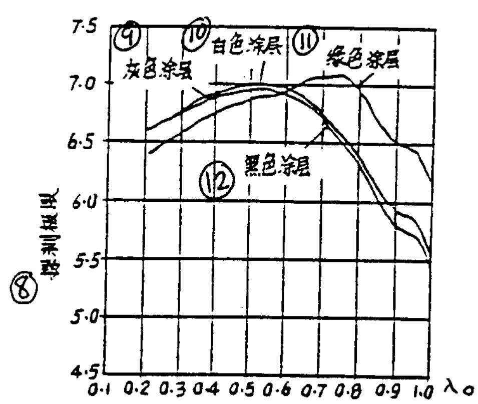


① 图 3 信噪比与 $\lambda_0$ 的关系

⑦ 图 4 探测极限与 $\lambda_0$ 的关系

**Key:** (1). Figure 3. The relationship between signal-to-noise ratio and $\lambda_0$. (2). Signal-to-noise ratio. (3). Painted gray. (4). Painted white. (5). Painted green. (6). Painted black. (7). Figure 4. The relationship between detection limits and $\lambda_0$. (8). Detection limits. (9). Painted gray. (10). Painted white. (11). Painted green. (12). Painted black.

## Reference Documents

1. W. Rerk, "Ground-based Electro-optical Surveillance of Satellites in Daylight by Detection of Reflected Sunlight." AD-All 7413, 1982.

2. [United States] Radio Corporation, Editors, *Electro-optics Handbook*, Beijing: National Defense Industry Publishing House, 1978.

3. F. Gelumu [probably a transliteration of "Groom"] et al., *Radiometry*, Beijing: Mechanical Engineering Publishing House, 1987.

4. Liu Jikun, *The Physical Basis for Solid-state Camera Devices*, Electronic Science and Technology University Publishing House, 1989.

5. R.H. Kingston, *Optical and Infrared Radiation Detection*, Beijing: Scientific Publishing House, 1984.

6. R. Weber, "The Limits of Detectability of Low-Light-Level Point-Source Sensors: A Function of Telescope Aperture, Sensor Resolution, Night-Sky Background, and Pre-readout Electron Gain." AD-785137, 1974.

7. Anhui Photomechanical Institute et al., *Determination of Visible Light Bidirectional Reflection Distribution of Surface Materials of Space Targets*. Internal materials.

## DISTRIBUTION LIST

## DISTRIBUTION DIRECT TO RECIPIENT

| ORGANIZATION | MICROFICHE |
|---|---|
| B085 DIA/RTS-2FI | 1 |
| C509 BALLOC509 BALLISTIC RES LAB | 1 |
| C510 R&T LABS/AVEADCOM | 1 |
| C513 ARRADCOM | 1 |
| C535 AVRADCOM/TSARCOM | 1 |
| C539 TRASANA | 1 |
| Q592 FSTC | 4 |
| Q619 MSIC REDSTONE | 1 |
| Q008 NTIC | 1 |
| Q043 AFMIC-IS | 1 |
| E404 AEDC/DOF | 1 |
| E410 AFDTC/IN | 1 |
| E429 SD/IND | 1 |
| P005 DOE/ISA/DDI | 1 |
| 1051 AFIT/LDE | 1 |
| P090 NSA/CDB | 1 |

Microfiche Nbr: FTD95C000789
NAIC-ID(RS)T-0638-95